Astron. Astrophys. 348, 542–552 (1999)

ASTRONOMY
AND
ASTROPHYSICS

Fundamental parameters of galactic luminous OB stars

III. Spectroscopic analysis of O stars in Cygnus OB2⋆

A. Herrero[1,2], **L.J. Corral**[1], **M.R. Villamariz**[1], **and E.L. Martín**[1,⋆⋆]

[1] Instituto de Astrofísica de Canarias, c/Vía Lactea s/n, E-38200 La Laguna, Tenerife, Spain
[2] Universidad de La Laguna, Departamento de Astrofísica, Avda. Astrofísico Francisco Sánchez, s/n, E-38071 La Laguna, Spain

Received 26 January 1999 / Accepted 4 May 1999

Abstract. We present the results of the spectral analysis of 11 OB stars in Cyg OB2, among them seven giants and supergiants. The projected rotational velocities of these stars are low or moderate. We find that only one of the stars (previously classified as luminosity class V) shows helium enhancement, and that this turns out to be compatible with standard evolutionary models without rotation. Only a second object gives an abundance that could be larger than solar. In addition, these two stars are found to be the most luminous in the sample. In summary, no helium discrepancy is found for the stars analysed in Cyg OB2. The cause of this result is speculated to be due to: a) the youth of the stars studied, b) the low rotational velocity of the sample observed, or c) a combination of both. The massive stars in Cyg OB2 are found to have ages between 1 and 5 Myr, and the most massive ones have initial evolutionary masses in excess of 100 $M_\odot$. Thus we confirm that Cyg OB2 is a young association rich in very massive stars. We study a possible correlation between the helium abundance and the stellar rotation and conclude that present data are consistent with the hypothesis that mixing processes probably related to rotation are present in the massive stars and in some cases strongly influence their early evolutionary phases.

Key words: stars: early-type – stars: atmospheres – stars: fundamental parameters – stars: evolution – stars: individual: Cyg OB2

1. Introduction

Massive hot stars are important constituents of galaxies and play a key role in their structure and evolution through their strong stellar winds and their own evolution (see Kudritzki, 1998; Leitherer, 1998). In order to understand the behaviour of massive hot stars it is necessary to get accurate parameters for them. These parameters are then used as input quantities for the theory of radiatively driven winds, in the study of the interstellar medium, the theory of stellar evolution and in the study of galactic evolution among other problems.

With this goal in mind Herrero et al. (1992; hereafter Paper I) carried out the first extensive analysis of massive OB stars in the Milky Way. They analysed with state-of-the-art methods 25 stars with spectral types from B0.5 to O5, and found a number of results, besides the derivation of the stellar parameters. Among the results of Paper I are what the authors called *mass and helium discrepancies*. The mass discrepancy consists of a difference between the masses predicted by the evolutionary theory on the one hand, and those predicted by the radiatively driven wind and the stellar photosphere theories on the other, differences larger than the adopted errors. The helium discrepancy consists of a difference between the surface helium abundances derived from the spectroscopic analysis and those predicted by the evolutionary theories, also beyond the adopted errors. These results have antecedents in the literature (see the references in the introduction of Paper I), although Herrero et al. were the first to give them a general character.

The discrepancies were found mainly for supergiants, although one of the supergiants was found to have a nearly normal helium abundance, and the stars rotating rapidly were found to have enhanced helium abundances even when they were of luminosity class V and lay close to the ZAMS. The mass discrepancy was shown to have a strong correlation with the distance from the Eddington limit. No mass or helium discrepancy was found for luminosity class V stars at low or moderate rotational velocities (although some authors extend the mass discrepancy to all luminosity class V objects; see, for example, Vacca et al., 1996, and references therein). No conclusion could be reached about whether the discrepancies were due to deficiencies in one of the theories or techniques involved, or in all of them.

The mass and helium discrepancies stimulated a number of studies in the field of stellar evolution and stellar atmospheres. Sellmaier et al. (1993), Herrero (1994), Schaerer & Schmutz (1994), Herrero et al. (1995) and de Koter et al. (1997), among others, have shown that the inclusion of sphericity and mass loss reduced the mass discrepancy by increasing the derived stellar gravity, but without solving the problem completely. Further-

Send offprint requests to: ahd@ll.iac.es

⋆ The Isaac Newton Telescope is operated on the island of La Palma by the RGO in the Spanish Obervatorio del Roque de los Muchachos of the Instituto de Astrofísica de Canarias.

⋆⋆ *Present address:* University of California, 601 Campbell Hall, Berkeley, CA 94270, USA

more, different studies of massive binaries do not clearly support any of the mass determinations (spectroscopic or evolutionary) against the other one (see Burkholder et al., 1997; Penny et al., 1998).

Recently, McErlean et al. (1998) and Smith & Howarth (1998) have shown that microturbulence strongly influences the helium lines in early B supergiants and late O supergiants, and thus that the helium discrepancy might be affected by it. Villamariz and Herrero (in preparation) confirm this result, but show that for O stars the corrected abundances are within the error bars given in Paper I. Thus the helium discrepancy cannot be completely explained by microturbulence.

On the side of the evolutionary theories, Langer (1992) proposed turbulent diffusion and semiconvection and Dennisenkov (1994) included rotationally induced diffusive mixing. Meynet & Maeder (1997), Maeder (1997), Talon et al. (1997), and Maeder & Zahn (1998) study rotational mixing induced by meridional circulation and turbulent diffusion. Langer & Heger (1998a, b) have studied the possibility of rotational velocity changes during stellar evolution and of evolution close to critical rotation. These studies show that by inclusion of additional mixing the stellar mass–luminosity relation and the surface abundances can be a function of the rotational velocity of the star and the stellar age. Thus, the position in the HRD would not uniquely determine stellar parameters, age and evolutionary status. Additional mixing seems to be a broad requirement over the HR diagram. For example, it has also been invoked as an explanation of the systematic age discrepancy between the conventional turnoff ages of young open clusters (Alpha Per, Pleiades) and the older ages derived from lithium observations of very low mass stars and brown dwarfs (Basri & Martín, 1999).

We thus decided to observe stars in an OB association, where we could study a more homogeneous sample than that used in Paper I. We have chosen the galactic association Cygnus OB2, which contains a wealth of OB stars. This association was studied by several authors in the past including Johnson & Morgan (1954), Schulte (1956, 1958), Lawrence & Redish (1965), Redish et al. (1967), Torres-Dodgen et al. (1990) and Massey & Thompson (1991). From the last authors we have taken new spectral type determinations from which we have selected the stars of our sample.

The observations are described in Sect. 2. In Sect. 3 we present the analysis of the spectra and the parameters that we derive from them. The discussion of the results is presented in Sect. 4 and in Sect. 5 we present the conclusions with some of the future work that can be done.

2. Observations

The observations were carried out by one of us (EM) with the 2.5 m Isaac Newton Telescope at the Roque de los Muchachos Observatory (La Palma) during a single observational run, in 1995 August. We observed the spectral region between 4000 and 5000 Å, and the region around H_α. The Intermediate Dispersion Spectrograph was used with the H 2400 B and the R 1200 B grids in the blue and the H 1800 V grid in the red, attached to the 235 mm camera, which resulted in a spectral resolution of 0.6, 1.2 and 0.8 Å, respectively, measured on the Cu–Ar arc. The wavelength coverage was different in the three cases: about 430 Å in the first case, 870 Å in the second, and 570 Å in the third. Thus, in the case of the H 2400 B grid we needed two exposures to cover the region of interest. Table 1 gives the stellar identification, position, magnitude, spectral type, and the spectral resolution obtained in the blue. Data are taken from Massey & Thompson (1991).

Table 1. Stars observed in Cyg OB2. All numerical identifications are taken from Schulte (1958), except for Cyg OB2 #516, which is taken from Massey & Thompson (1991). Positions for epoch 1950.0 have been taken from these last authors and processed within IRAF for epoch 2000.0. Spectral types are also from Massey & Thompson, except for Cyg OB2 #11 and #4, that are taken from Walborn (1973)

Ident	α(2000)	δ(2000)	V mag.	Spec. type	Blue resolution (Å)
22	20:33:08.8	41:13:17.8	11.55	O4 III(f)	1.3
516	20:33:23.5	41:09:12.0	11.84	O5.5 V((f))	1.3
8c	20:33:18.0	41:15:31.1	10.19	O5 If	1.3
9	20:33:10.8	41:18:07.9	10.96	O5 If	1.3
11	20:34:08.6	41:36:59.6	10.03	O5 If^+	1.3
29	20:34:13.5	41:35:02.4	11.91	O7 V	1.3
4	20:32:13.8	41:27:13.9	10.23	O7 III((f))	1.3
20	20:31:49.7	41:28:27.5	11.52	O9.5 V	0.6
19	20:33:39.1	41:19:25.9	11.07	O9.5 III	0.6
10	20:33:46.1	41:33:01.4	9.88	O9.5 I	0.6
21	20:32:27.8	41:28:53.4	11.42	B0.5 V	0.6

The usual reduction procedure of bias subtraction, flat-field division and wavelength calibration was applied using IRAF[1]. The spectra were rectified using our own procedure written in IDL in order to get normalized spectra that were compared to the results of atmospheric models (see Sect. 3).

Fig. 1 shows the blue spectra of the observed stars. We see the strong reddening in Cyg OB2 reflected in the intense IS absorption features at ∼4430 and ∼4880 Å. The stars were selected in an attempt to cover a significant range in luminosity and temperature on the HRD, but without aiming at a complete sample.

3. Spectral analysis

Before doing the comparison with the theoretical model atmospheres, we determined rotational velocities following the same procedure indicated in Paper I. Rotational velocities are given in Table 2 together with the parameters determined for each star. We see that all O stars show low or moderate projected rotational velocities. Furthermore, six out of the eleven stars have very similar projected rotational velocities, between 120 and 140 km s^{-1}.

[1] The IRAF package is distributed by the National Optical Astronomy Observatories, which is operated by the Association of Universities for Research in Astronomy, Inc., under contract with the National Science Foundation.

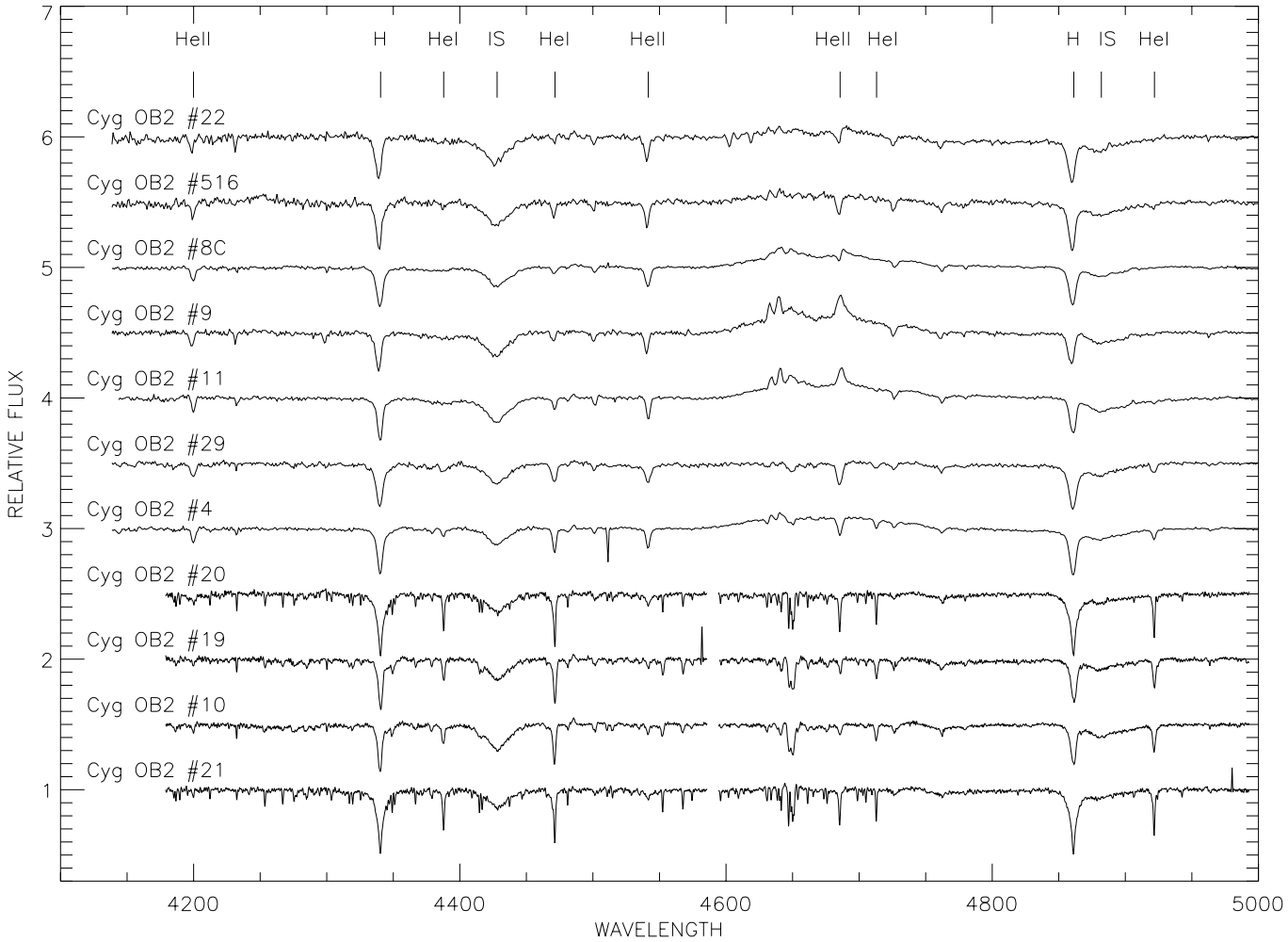

Fig. 1. The blue stellar spectra. The relative fluxes have been arbitrarily displaced in steps of 0.5 for the sake of clarity. At the top, the main lines used in the analysis are marked, together with the IS bands. Wavelengths are in Å.

The parameter determination was made following the procedure pointed out in Paper I, based on the analysis of the lines chosen in that work, namely H_γ, H_β, He I$\lambda\lambda$ 4387, 4922, 4471 and He II$\lambda\lambda$ 4199, 4541 Å. Here, we give an overview of the method.

The spectral line profiles of H, He I and He II were compared with the line profiles synthesized for a large set of NLTE plane–parallel, hydrostatic model atmospheres calculated without line-blocking (see Paper I for details). The models were calculated from 25 000 to 50 000 K in $T_{\rm eff}$, in steps of 2 000 K, between 3.0 and 4.4 in $\log g$, in steps of 0.2 dex, and for two values of the helium abundance by number, ϵ = 0.09 and 0.20 (where $\epsilon = N({\rm He})/N({\rm He}) + N({\rm H})$).

For each spectral line of H, He I and He II, we find the combinations of $\log g$ and $T_{\rm eff}$ that best fit the whole line profile (not only the equivalent width), and we plot the resulting fitting curve in the $\log g$–$T_{\rm eff}$ plane. The parameters of the star are given by the intersection of these curves for all the lines used in the analysis, which is ideally a single point for the right value of ϵ, but actually it is an area of the diagram whose center we assume to give the parameters of the star. The procedure is made at the two helium abundances and an interpolation is made in ϵ, adopting the ϵ with the smallest intersection region as the stellar helium abundance. The size of the region of line intersection is adopted as the intrinsic error of the parameters. Usually the errors found are of $\pm$ 1 500 K in T and $\pm$ 0.1 in $\log g$. There is no strong dependence on resolution, because we use here only the relatively broad lines of H and He.

Following these procedures preliminary parameters were derived for each star. From here on we calculate new models changing $T_{\rm eff}$, $\log g$ and ϵ as the fits to the lines suggest, until we find the best fit to the observed spectra, which gives us the final parameters of the star.

In this second step of the analysis we decided to introduce line-blocking in the model profile calculations. Line-blocking was shown by Herrero (1994) to be responsible for the discrepancy found in Paper I between the $T_{\rm eff}$ values derived from singlet and triplet He I lines above 40 000 K. We have included line-blocking in an approximate way by treating the metal populations in LTE. As a result of the inclusion of line-blocking the UV flux is diminished, and the model that best fits the profiles differs from that calculated without line-blocking. A more de-

tailed discussion can be found in Herrero et al. (in preparation). The differences were always smaller than 1 500 K in $T_{\rm eff}$. All these calculations were made without microturbulence, as the results of Villamariz & Herrero (in preparation) show that the inclusion of this parameter has only a minor effect for models in the O-star region.

In Figs. 2 to 12 we present the comparison of the observed and calculated profiles. With the parameters obtained we calculate radii, luminosities and gravities corrected for the effect of centrifugal forces and spectroscopic masses, in the same way we followed in Paper I. The absolute magnitudes have been taken from Massey & Thompson (1991).

The final parameters derived for the observed stars are presented in Table 2.

3.1. Comments on individual stars

Here we comment on some difficulties or inconsistencies we have found in the data, the analysis or the results of each particular object.

Cyg OB2 #22 The spectral-line fits of this star can be seen in Fig. 2. The line fit is impossible for the singlet He I lines. They are too weak and get lost in the noise of the continuum. At this high temperature, however, the He I 4471 line should be reliable. The preferred model has a moderate He enhancement. The age we derive for this star is very low, even less than 1 Myr.

Cyg OB2 #516 The star has been classified as O5.5 V((f)) by Massey & Thompson (1991). The reddening given by these authors is very large, and thus the absolute magnitude derived from the distance modulus is –6.89, much larger than that corresponding to its spectral classification. The discrepancy is less worrying if we consider the low value found for the gravity, more typical for a giant than for a dwarf. If Cyg OB2 #516 has stellar parameters closer to typical giants than to dwarfs, its absolute magnitude would be less than one magnitude brighter than the canonical value for this spectral type (Massey, 1998, gives –5.9 mag as the $M_{\rm v}$ value of an O5.5 III star). Even then, Cyg OB2 #516 would be very luminous and would be among the most luminous stars in the Milky Way. Such large departures from the correlation between spectral classification and stellar parameters can be expected if the chemical composition of the atmosphere is also non-standard. Interestingly enough, Cyg OB2 #516 is the only star in our sample for which we have derived an enhanced helium abundance. The spectral-line fit is relatively bad for He I 4387, but trying to improve it would not help to reduce the high helium abundance. Nevertheless, this value is coincident with the predictions of the evolutionary tracks by Schaller et al. (1992), which give ϵ= 0.14 for this star. Thus, no helium discrepancy is found for this object. Also interesting is that it does not show a clear mass discrepancy, and that both the spectroscopic and evolutionary masses are close to or above the 100 $\rm M_{\odot}$ value. The spectral-line fits can be seen in Fig. 3.

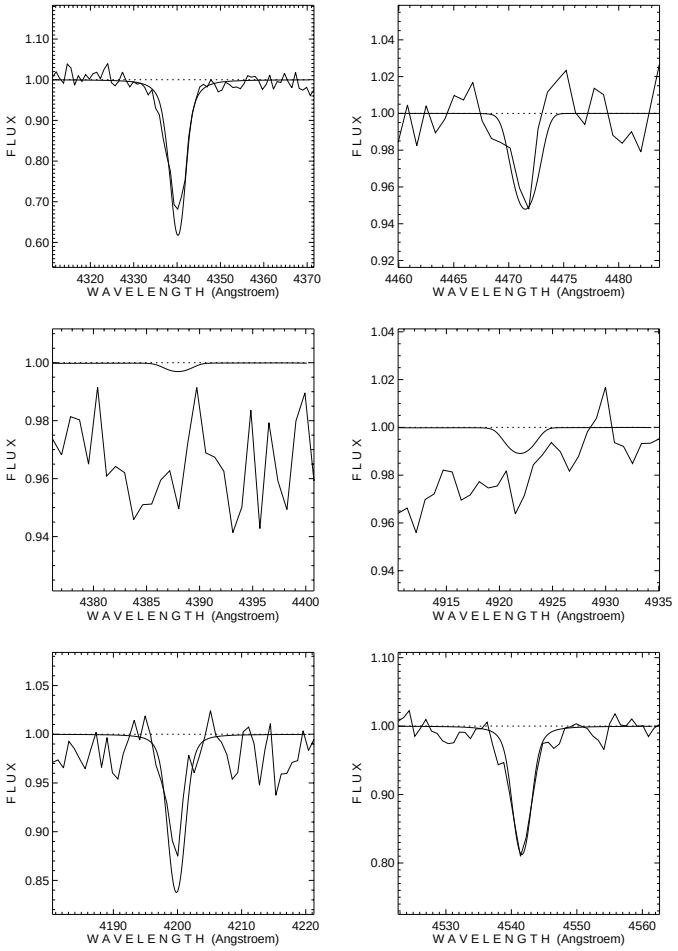

Fig. 2. The spectral-line fits for Cyg OB2 #22. From left to right and top to bottom, we show the fits of $\rm H_{\gamma}$, He I 4471, He I 4388, He I 4922, He II 4200 and He II 4541 for the model with $T_{\rm eff}$ = 47 000 K, $\log g$= 3.60 and ϵ= 0.12. Note that the vertical scale is different for different lines.

Cyg OB2 #8C The star has been classified as an O5 If star. However, we derive a relatively high gravity, although the mass discrepancy is large. The line fit of He I 4387 is again impossible, and the continuum near He I 4922 presents difficulties for the rectification due to the strong IS absorption, so that the line has not been used for the parameter determination. The spectral-line fits can be seen in Fig. 4.

Cyg OB2 #9 The spectral-line fits shown in Fig. 5 indicate that the plane–parallel gravity could be slightly lower. The He I singlet lines have similar problems to those of #22 and #8C. There is a problem with the distance of this star. *Hipparcos* has measured a parallax of 2.48 $\pm$ 1.75 mas, corresponding to a distance of 403 pc, with minimum and maximum distances of 235 and 1430 pc. On the other hand, Massey & Thompson (1991), in agreement with other authors, give a distance modulus of 11.17 $\pm$ 0.08, which corresponds to a distance of 1713 $\pm$ 65 pc. Thus, there is some doubt that Cyg OB2 #9 belongs to the cluster. However, the reddening data are perfectly compatible with those

Table 2. Parameters determined for the programme stars. The second column gives the spectral type. Temperatures are given in thousands of kelvin; gravities are corrected for centrifugal force effects; ϵ is the helium abundance by number; V is the integral of the stellar flux over λ, weighted by the V-filter function of Matthews & Sandage (1963), used to calculate stellar radii from the model atmospheres (see Kudritzki, 1980, or Paper I); $M_{\rm s}$, $M_{\rm ev}$ and M_0 are the spectroscopic mass, the present evolutionary mass and the initial evolutionary mass, respectively. The latter have been obtained from the evolutionary tracks by Schaller et al. (1992) for non-rotating stars.

Star	S.T.	$T_{\rm eff}$	$\log g$	ϵ	$V_{\rm r} \sin i$	V	$M_{\rm v}$	$R/R_\odot$	$\log(L/L_\odot)$	$M_{\rm s}$	$M_{\rm ev}$	M_0
22	O4 III(f)	47.0	3.61	0.12	125	–29.482	–6.69	22.7	6.36	76.2	118.7	131
516	O5.5 V((f))	44.0	3.61	0.15	135	–29.449	–6.89	25.2	6.33	94.5	100.1	123
8c	O5 If	48.0	3.77	0.09	145	–29.555	–5.61	13.3	5.93	37.8	73.1	74
9	O5 If	44.5	3.52	0.09	135	–29.390	–6.53	22.0	6.24	57.5	98.9	107
11	O5 If$^+$	43.0	3.42	0.09	120	–29.327	–6.51	22.4	6.17	47.5	80.7	94
29	O7 V	40.0	3.83	0.09	180	–29.390	–4.71	9.5	5.32	22.3	34.2	35
4	O7 III((f))	39.0	3.52	0.07	125	–29.301	–5.44	13.9	5.60	23.2	42.1	44
20	O9.5 V	35.0	4.00	0.09	25	–29.221	–3.88	7.0	4.82	17.9	21.8	22
19	O9.5 III	30.0	3.02	0.09	75	–28.904	–5.41	16.4	5.29	10.3	26.7	28
10	O9.5 I	31.0	3.11	0.09	85	–28.930	–6.86	31.6	5.92	46.9	54.2	61
21	B0.5 V	34.5	3.90	0.09	30	–29.160	–3.58	6.3	4.70	11.4	20.2	21

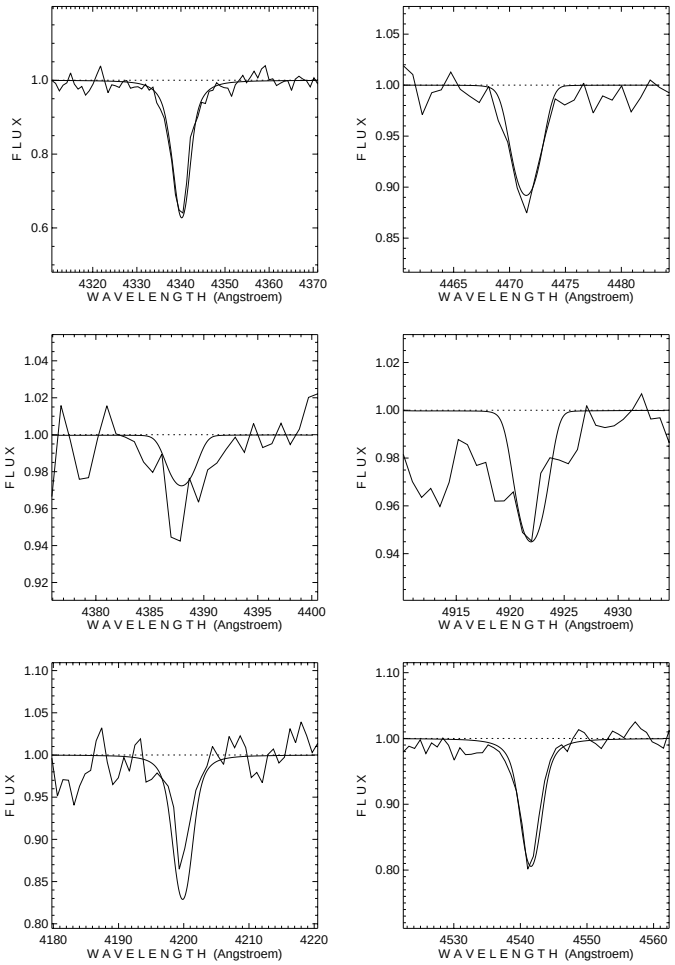

Fig. 3. The spectral-line fits for Cyg OB2 #516, with $T_{\rm eff}$= 44 000 K, $\log g$= 3.60 and ϵ= 0.15. The order of the lines shown is the same as in Fig. 2. Note that the vertical scale is different for different lines.

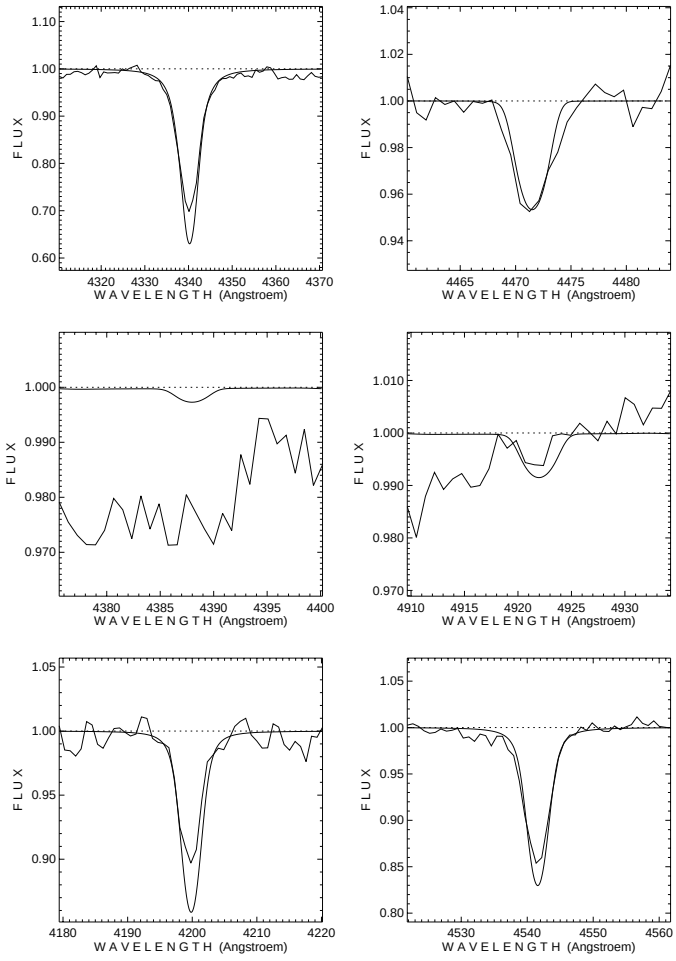

Fig. 4. The spectral-line fits for Cyg OB2 #8C, with $T_{\rm eff}$= 48 000 K, $\log g$= 3.75 and ϵ= 0.09. The order of the lines shown is the same as in Fig. 2. Note that the vertical scale is different for different lines.

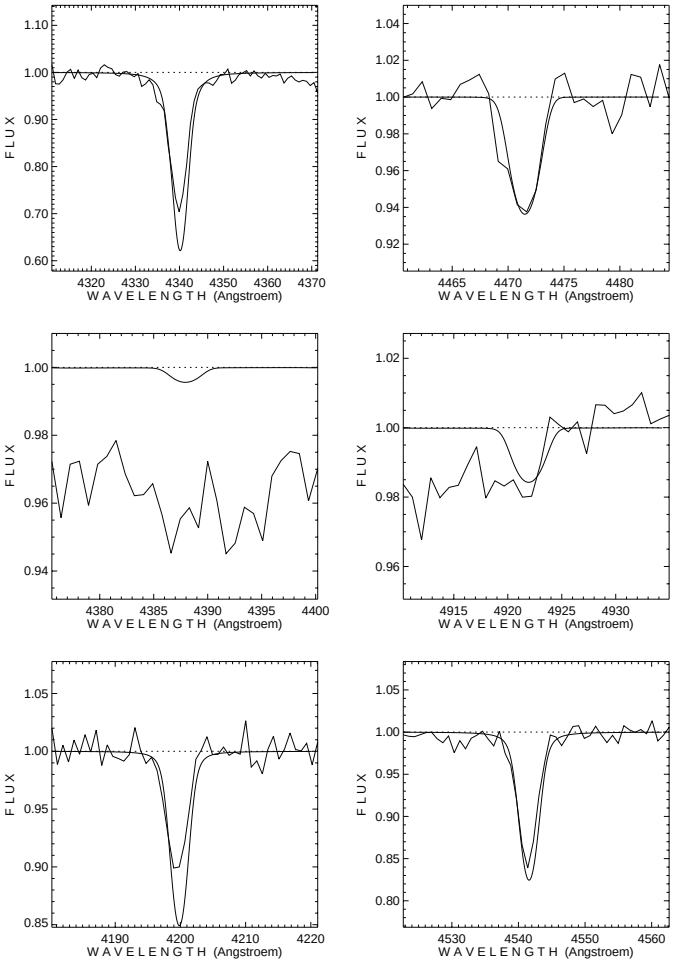

Fig. 5. The spectral-line fits for Cyg OB2 #9, with $T_{\rm eff}$= 44 500 K, $\log g$= 3.50 and ϵ= 0.09. The order of the lines shown is the same as in Fig. 2. Note that the vertical scale is different for different lines.

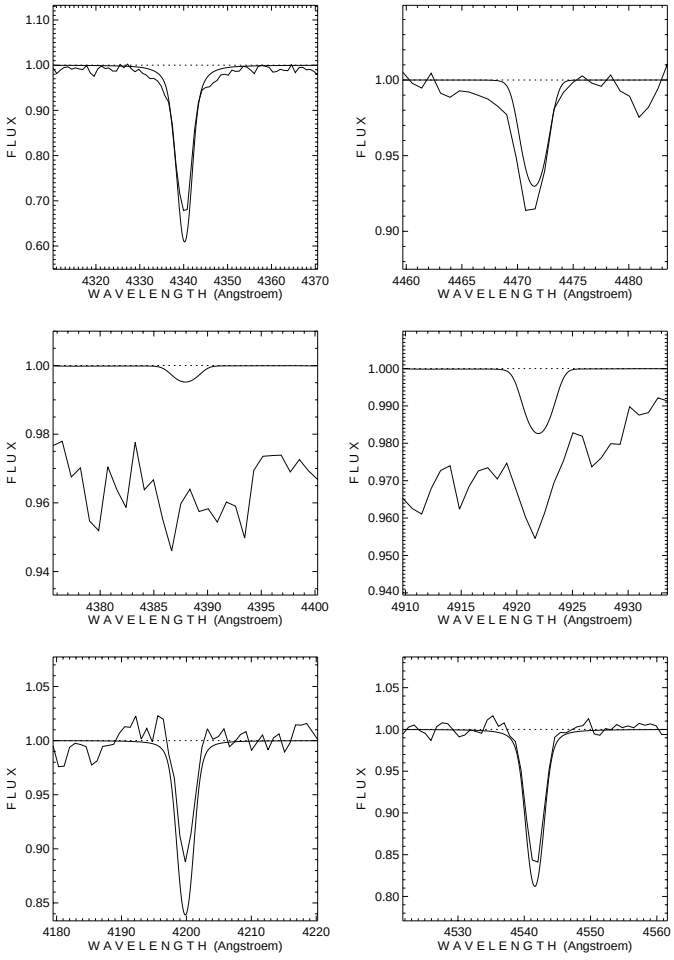

Fig. 6. The spectral-line fits for Cyg OB2 #11, with $T_{\rm eff}$= 43 000 K, $\log g$= 3.45 (although the best fit is with $\log g$= 3.40, see text) and ϵ= 0.09. The order of the lines shown is the same as in Fig. 2. Note that the vertical scale is different for different lines.

of all other stars in the cluster. Thus we prefer to assume that Cyg OB2 #9 belongs to the cluster.

Cyg OB2 #11 The adopted model, with a log g of 3.40 could not be brought to convergence. Instead, we show in Fig. 6 the fit of the next converged model, with $\log g$= 3.45, all other parameters being the same.

Cyg OB2 #29 The spectral-line fits are shown in Fig. 7. We see that now the He I 4922 fits slightly worse than the other two He I lines, but all three are consistent within the errors.

Cyg OB2 #4 The derived He abundance is ϵ= 0.07, slightly lower than solar. Again, the main conclusion is that the star does not seem to be He enriched, in spite of being an O giant.

Cyg OB2 #20 The spectral-line fits are shown in Fig. 9. Only He II 4200 seems to show a problematic fit. The value of the visual extinction, $A_{\rm V}$, given in Massey & Thompson (1991) corresponds to an R value of 2.42, much lower than the standard value or the average value of 3.0 derived from all other Cyg OB2 stars (see Table 7 in Massey & Thompson, 1991). This low value leads to an absolute magnitude of –3.06, which would correspond to a much cooler star (later than B1 V). This would again lead to very small values of the radius and mass. Massey & Thompson (1991) do not discard the star as a member of Cyg OB2. Thus we have adopted the average value of R = 3.0 and derived all values from here. The obtained values, which we could define as *normal* for an O9.5 V star, are those given in Table 2.

Cyg OB2 #19 The spectral-line fits are shown in Fig. 10. In spite of the low gravity, the fit is consistent with a normal He abundance. Furthermore, if we try to give more weight to He I 4387 (taking into account that this line is only weakly affected by microturbulence, see McErlean et al., 1998, and Smith & Howarth, 1998), the helium abundance would be lower. This case is similar to others found in Paper I, where He I 4922 was preferred to He I 4387 because this last would indicate He abun-

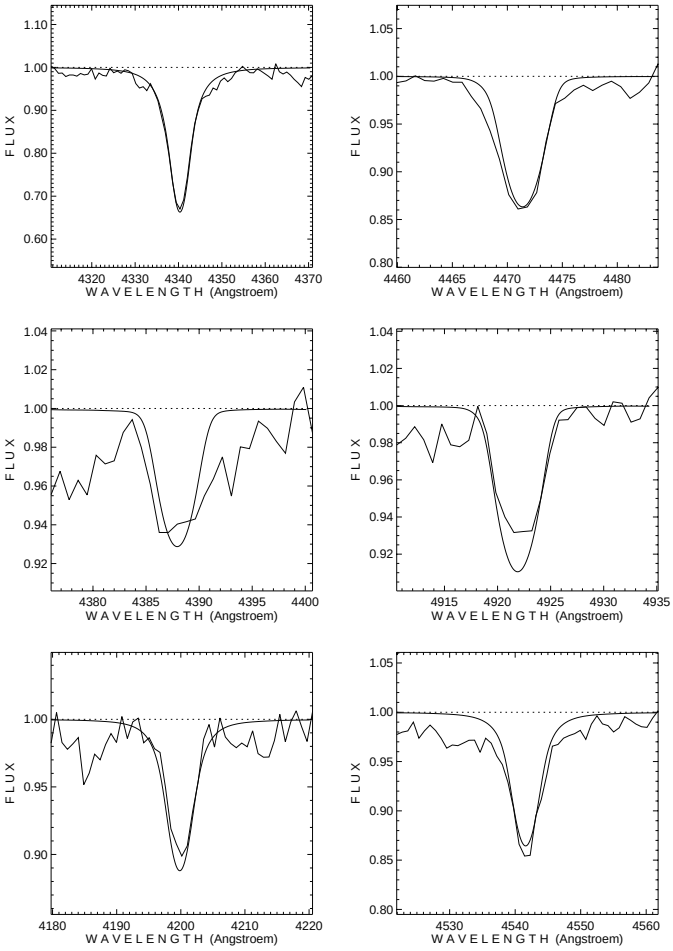

Fig. 7. The spectral-line fits for Cyg OB2 #29, with $T_{\rm eff}$= 40 000 K, $\log g$= 3.80 and ϵ= 0.09. The order of the lines shown is the same as in Fig. 2. Note that the vertical scale is different for different lines.

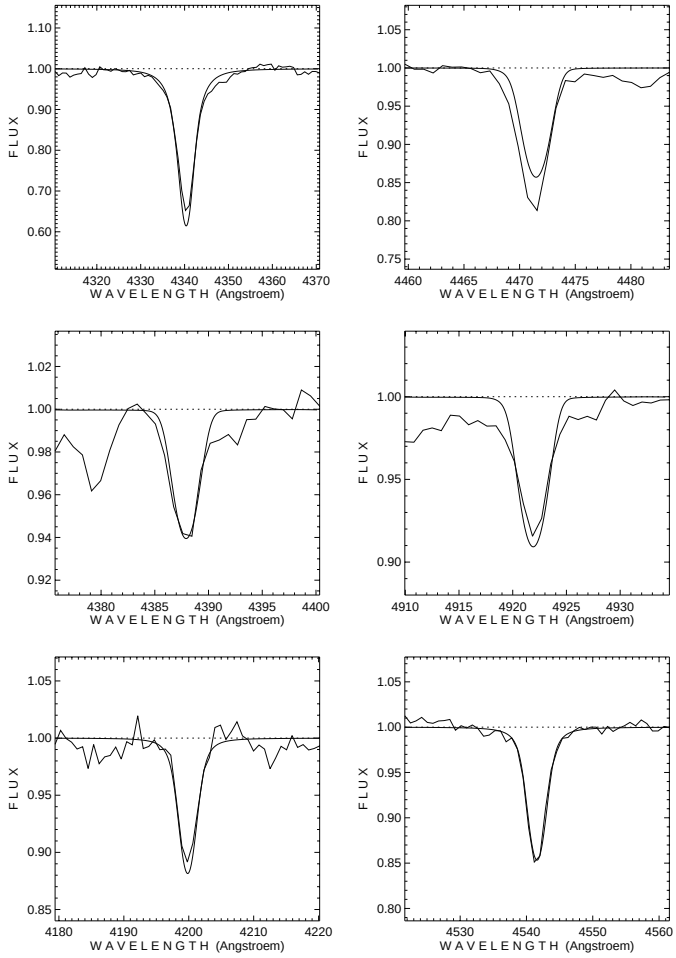

Fig. 8. The spectral-line fits for Cyg OB2 #4, with $T_{\rm eff}$= 39 000 K, $\log g$= 3.50 and ϵ= 0.07. The order of the lines shown is the same as in Fig. 2. Note that the vertical scale is different for different lines.

dances lower than solar. The important point for the present analysis is that the star, being a late O supergiant, is not helium enriched.

Cyg OB2 #10 As for Cyg OB2 #19 we have chosen the best fit given by He I 4922 (see Fig. 11). Again, this will not affect the conclusion that the star is not He enriched.

Cyg OB2 #21 The spectral-line fits are shown in Fig. 12. Only the He II 4200 line seems to be slightly problematical.

4. Discussion

In Paper I a correlation was found between the mass discrepancy and the distance from the Eddington limit. This correlation was attributed to the use of plane–parallel, hydrostatic models, and thus it is not surprising that we find it again in the present data, as can be seen in Fig. 13. As has been said in the introduction, the inclusion of sphericity and mass loss in the models significantly reduces the mass discrepancy (see Herrero et al., 1995, and Herrero et al., in preparation, for more detailed discussions). Thus we will not investigate the mass discrepancy further here. Instead, we will concentrate on the helium discrepancy.

The easiest way to show that the helium enhancement is related to the rotational velocity would be to find a tight correlation between rotational velocity and helium abundance, or better, between $\omega = \Omega/\Omega_{\rm crit}$ (where Ω is the equatorial angular velocity at the stellar surface and $\Omega_{\rm crit}$ is the corresponding break-up velocity, including the effect of radiation pressure, for which we have used the approximate expression VII.7 given in Kudritzki, 1988), which is the parameter affecting the stellar evolution (see Meynet & Maeder, 1997, Maeder, 1997, Maeder & Zahn, 1998) and the helium abundance. In Fig. 14 we have represented the values we have obtained here and in Paper I, plus values from Herrero et al. (1995), Herrero et al. (in preparation) and Israelian et al. (priv. communication). It is difficult to see any correlation.

However, with stars taken from different clusters and from the field this would be very hard. To illustrate this point, let us imagine that there exists a clear relation between helium abundance and ω of the form

$$\epsilon = a_0 + a_1\omega + a_2\omega^2.$$

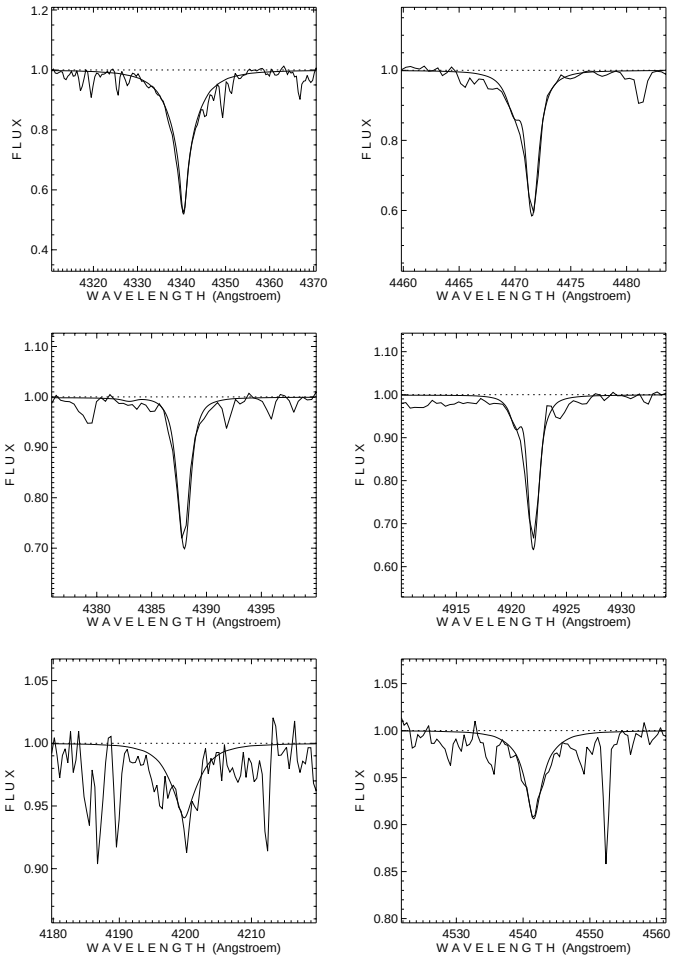

Fig. 9. The spectral-line fits for Cyg OB2 #20, with $T_{\rm eff}$= 35 000 K, $\log g$= 4.00 and ϵ= 0.09. The order of the lines shown is the same as in Fig. 2. Note that the vertical scale is different for different lines.

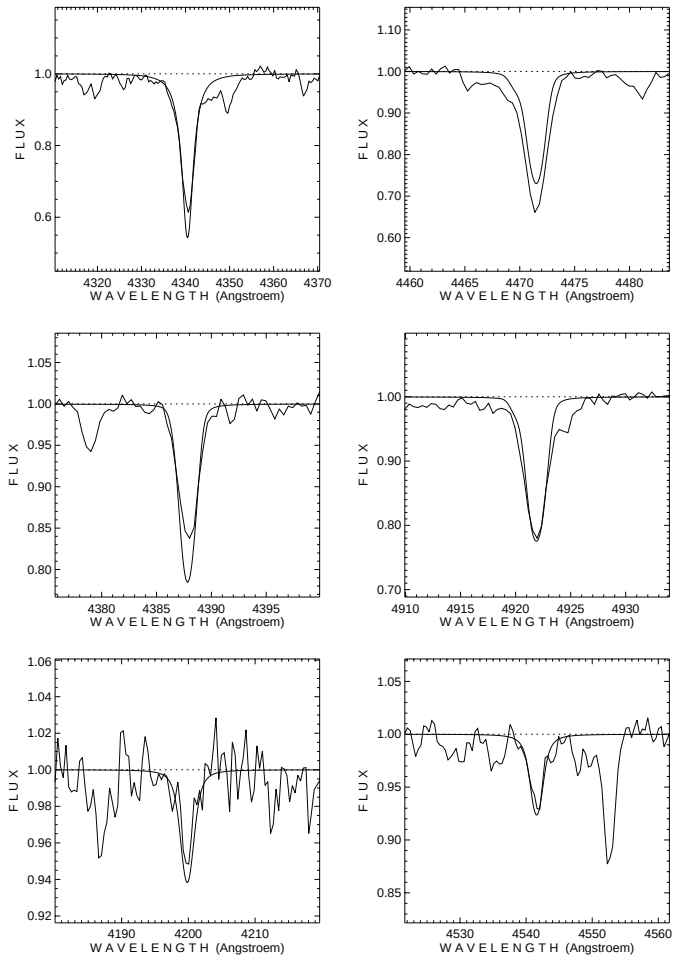

Fig. 10. The spectral-line fits for Cyg OB2 #19, with $T_{\rm eff}$= 30 000 K, $\log g$= 3.00 and ϵ= 0.09. The order of the lines shown is the same as in Fig. 2. Note that the vertical scale is different for different lines.

To find the coefficients of the formula let us arbitrarily assume that the stars with the larger ω at a given ϵ in the data of Fig. 14 have a negligible projection effect. Then we obtain a_0 = 0.10, a_1 = -0.12 and a_2 = 0.39.

Now we try to determine the real distribution of ω among the O stars. For this, we take advantage of the data of projected rotational velocities published by Howarth et al. (1997). For those stars with good data and known spectral type, we construct the distribution function of observed projected rotational velocities. The spectral types are then used to calculate ωsin(i) using the calibration of stellar parameters versus spectral type given by Howarth & Prinja (1989). (We have to use this calibration because we do not have individual data for all the stars considered). Then we use Lucy's algorithm (Lucy, 1974) to obtain the intrinsic distribution of ω under the assumption that the stellar rotational axes are randomly distributed in space. Fig. 15 illustrates both the observed and the intrinsic distributions.

Having the intrinsic distribution of ω we generate a sample of 10 000 points according to such a distribution and use the expression above to assign them helium abundances. In this form we have a simulated sample of O stars that we now project according to a random orientation of their rotational axes with respect to our line of sight. The resulting diagram of helium abundances versus ω sin(i) is shown in Fig. 16. It is easy to see that if we pick up a few stars at random (i.e., not chosen because of their velocities or helium abundances) we will end up with a distribution similar to that from Fig. 14. In addition, effects like progressive enrichment (mixing does not necessarily occur instantaneously, the He enrichment needs time to appear) and rotational velocity changes (see for example Langer & Heger, 1998a, b) are very likely and will tend to hide the original dependence. Of course, Fig. 16 is not a proof of any law relating ϵ and ω, but shows that the observed data are not incompatible with such a relation.

Our Cyg OB2 sample consists of eleven stars, seven of which had been classified as giants or supergiants. None of the last has shown the enhancement in the helium abundance that was found in Paper I for this kind of stars, although we have followed the same techniques and criteria (except for the inclusion of line-blocking effects, which does not affect the results beyond the error bars, see Herrero et al., in preparation). In view of the above discussions concerning the helium abundances and rota-

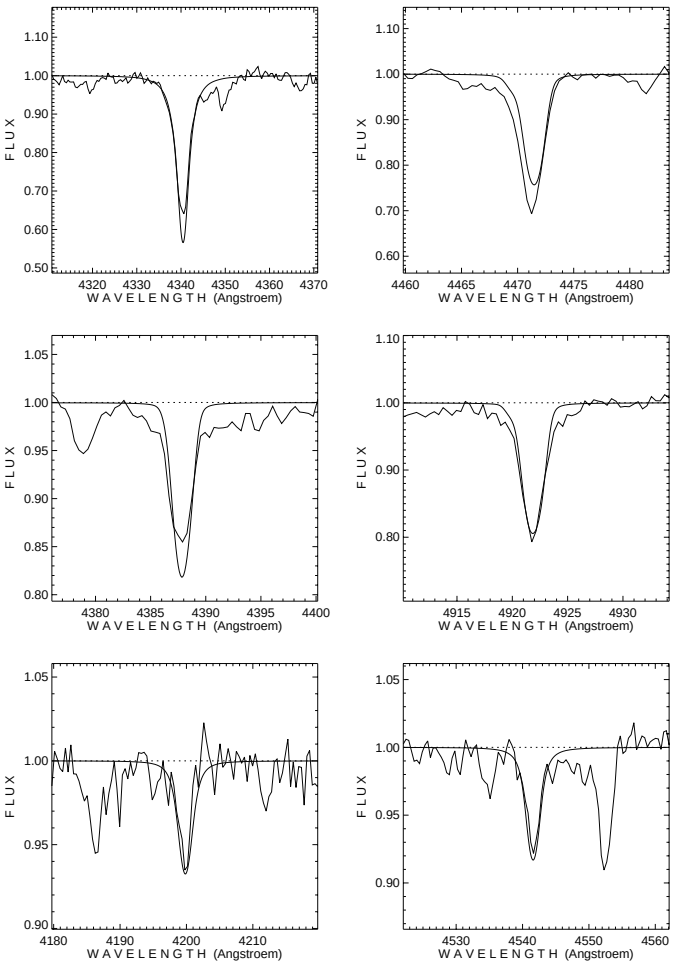

Fig. 11. The spectral-line fits for Cyg OB2 #10, with $T_{\rm eff}$= 31 000 K, $\log g$= 3.10 and ϵ= 0.09. The order of the lines shown is the same as in Fig. 2. Note that the vertical scale is different for different lines.

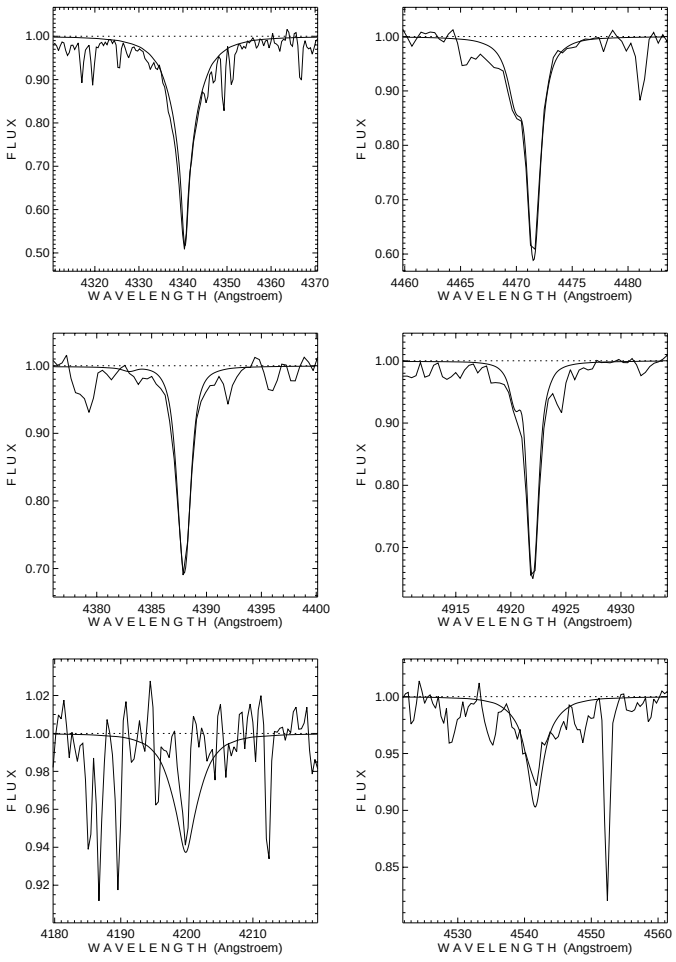

Fig. 12. The spectral-line fits for Cyg OB2 #21, with $T_{\rm eff}$= 34 500 K, $\log g$= 3.90 and ϵ= 0.09. The order of the lines shown is the same as in Fig. 2. Note that the vertical scale is different for different lines.

tional velocities, this is a very interesting result. In addition, the only star for which we derive a helium enhancement is classified as luminosity class V (although its gravity and other properties would allow us to include it among the giants, see the notes in the preceding section). This star seems to be extremely luminous, and thus it could be that the enhanced helium is an effect of a faster evolution. This possibility is confirmed by the fact that the evolutionary tracks of Schaller et al. (1992) predict a surface helium abundance of ϵ= 0.14 for this star. We should note, however, that a larger efficiency of a hypothetical mixing mechanism would also increase the abundance. Interestingly, the only other one star for which we find indications of helium enhancement is also very luminous. We can see in the HR diagram of Fig. 17 that both stars lie close to each other, and that they are the most luminous stars in the sample. Also their projected rotational velocities are similar.

The most promising working hypothesis we can think of is that the low rotational velocities or the youth of the stars in Cyg OB2, or both combined, are avoiding the effect of mixing mechanisms on the surface helium abundance, and that only for the most luminous stars are these mechanisms efficient enough

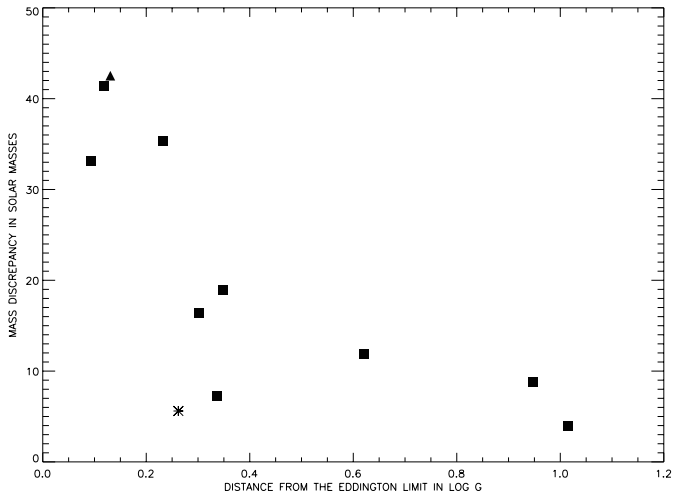

Fig. 13. The mass discrepancy in Cyg OB2 with the data from Table 2. The stars that could be helium enhanced are represented by an asterisk (Cyg OB2 #516) and a triangle (Cyg OB2 #22); stars with normal helium abundances are represented by filled squares.

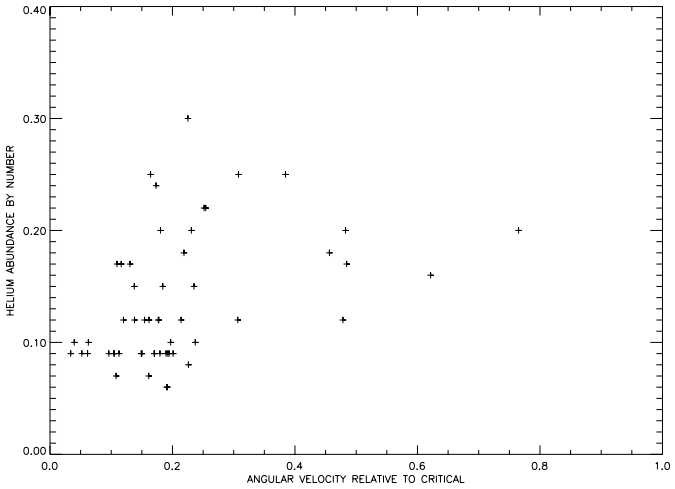

Fig. 14. The helium abundance plotted against the observed projected fractional angular velocity ($\omega = \Omega \sin(i)/\Omega_{\rm crit}$); for stars analysed in Paper I, in Herrero et al. (1995, in preparation) and here

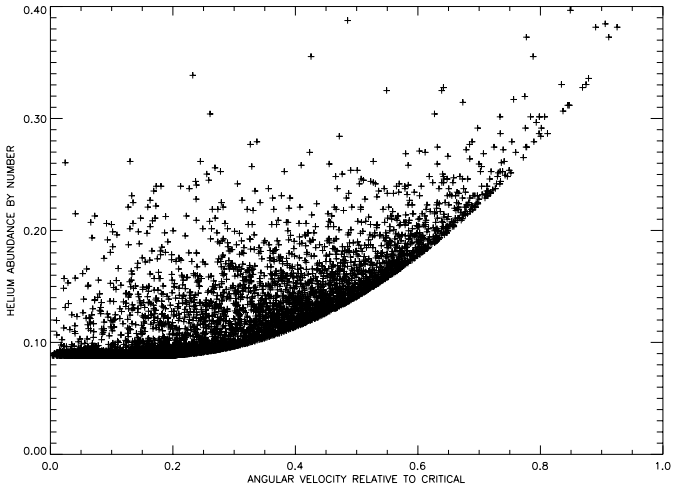

Fig. 16. Simulation of the dependence of the helium abundance on the projected rotational velocity for stars following the law given in the text. Compare the results of randomly picking up a few stars from this figure with the observed distribution from Fig. 14.

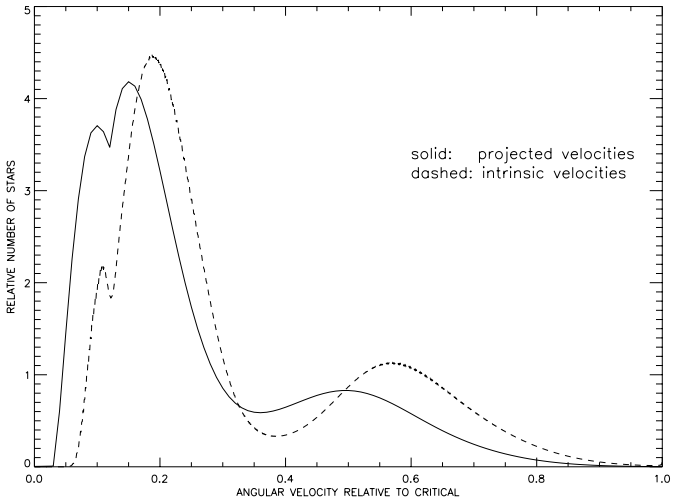

Fig. 15. The observed distribution of ω sin(i) compared to the intrinsic one. Observed rotational velocities (projected) are taken from Howarth et al. (1997), and the spectral type–stellar parameters calibration of Howarth & Prinja (1989) has been adopted. The inversion has been performed with Lucy's algorithm (Lucy, 1974).

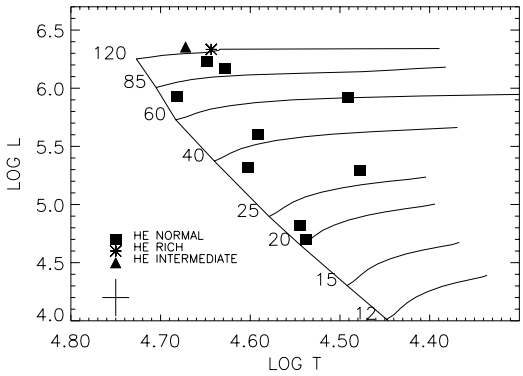

Fig. 17. The HR diagram of the stars analysed in Cyg OB2. The cross at the bottom left corner represents error bars. Numbers in the diagram represent initial evolutionary masses. Tracks are from Schaller et al. (1992) for non-rotating stars.

or the evolutionary timescales short enough to affect the photospheric abundances. However, it is impossible to demonstrate these hypotheses with only the present data for Cyg OB2, and we will need to explore more galactic OB associations before reaching firm conclusions.

Note that, except for the approximate inclusion of line-blocking effects, we have not changed or improved our model atmospheres with respect to the calculations in Paper I, nor have we changed the reduction and analysis techniques. Thus, all the cautionary remarks made in Paper I, in the sense that we cannot discard the possibility that the helium discrepancy is due to deficiencies in the model atmospheres or in the spectroscopic analysis techniques remain valid. What we can state is that the present data are compatible with the hypothesis that mixing processes probably related to rotation are present in massive stars and in some cases strongly influence their early evolutionary phases.

Finally, let us say a few words about the association. From the points in Fig. 17 we see that Cyg OB2 contains some very young stars, with initial masses above 100 $\mathrm{M}_{\odot}$. Indeed, if we derive the age from these stars, we would see that their positions are compatible with an age of about 1.0–1.5 Myr. (derived from the tracks by Schaller et al., 1992), much younger than the minimum age of 3 Myr. given by Torres-Dodgen et al. (1990) for Cyg OB2. However, as we see in Fig. 17, a few of the stars (Cyg OB2 #10 and #19) suggest a greater age, of 3–5 Myr. We should point out that we have not seen signs of binarity in the spectra of these last stars that could alter their evolution. This is

consistent with the finding by Massey & Thompson (1991) that the stars in Cyg OB2 cannot be strictly coeval. Thus, it would be more correct to conclude that our data give an age of between 1 and 5 Myr for the massive stars in Cyg OB2 if we apply models for non-rotating stars.

5. Conclusions and future work

We have presented observations and analyses of 11 stars in Cyg OB2, a very young OB association. Seven of the stars were previously classified as luminosity class III or I, and we think that one more, Cyg OB2 #516, could also be classified as giant.

We find that the rotational velocities of the Cyg OB2 stars are all moderate (for O stars), a fact that could be very useful for investigating the helium discrepancy.

Only the most luminous stars in Cyg OB2 show indications of helium enhancements, but without showing a He discrepancy (i.e., the He abundances obtained from the spectroscopic analysis and from the evolutionary tracks agree). As a working hypothesis, we attribute this difference with the results found in Paper I to the moderate projected rotational velocities of the stars in Cyg OB2 and their low age. We cannot, however, conclusively demonstrate this hypothesis, and more analyses in other associations with a range in age and rotational velocities will be needed.

We confirm that Cyg OB2 is an association rich in massive stars. We find that three of the analysed stars have initial evolutionary masses in excess of 100 $M_\odot$, with spectroscopic masses that greatly exceed 50 $M_\odot$. The association is very young, and, applying evolutionary models for non-rotating stars, we find that there is an age spread in the massive stars of Cyg OB2 between 1 and 5 Myr.

No progress has been made here in explaining the mass discrepancy or in discarding the possibility that the helium discrepancy is due to deficiencies in any of the stages of the spectroscopic analysis. For this, we still have to improve our model atmospheres to include line-blanketing, sphericity, mass loss and turbulent motions in a self-consistent way. Different authors have already incorporated some of these effects in their models (see Sellmaier et al., 1993; Schaerer & Schmutz, 1994; Hubeny & Lanz, 1995; de Koter et al., 1997; Santolaya–Rey et al., 1997) and future analyses will have to consider a larger space of parameters. However, present data are compatible with the hypothesis that mixing processes probably related to rotation are present in the massive stars and strongly influence in some cases their early evolutionary phases.

Acknowledgements. We would like to thank Prof. A. Maeder and Prof. P. Massey for very useful comments about the manuscript. LJC wants to thank the CONACYT (Mexico) for a postdoctoral grant at the IAC. This work has been supported by the spanish DGES under project PB97-1438-C02-01.

References

Basri G., Martín E.L., 1999, ApJ 510, 266
Burkholder V., Massey P., Morrell N., 1997, ApJ 490, 328
de Koter A., Heap S.R., Hubeny I., 1997, ApJ 477, 792
Dennisenkov P.A., 1994, A&A 287, 113
Herrero A., 1994, Space Sci. Rev. 66, 137
Herrero A., Kudritzki R.P., Vílchez J.M., et al., 1992, A&A 261, 209 (Paper I)
Herrero A., Kudritzki R.P., Gabler R., Vílchez J.M., Gabler A., 1995, A&A 297, 556
Howarth I.D., Prinja R.K., 1989, ApJS 69, 527
Howarth I.D., Siebert K.W., Hussain G.A., Prinja R.K., 1997, MNRAS 284, 265
Hubeny I., Lanz T., 1995, ApJ 439, 875
Johnson H.L., Morgan W.W., 1954, ApJ 119, 344
Kudritzki R.P., 1980, A&A 85, 174
Kudritzki R.P., 1988, In: Chmielewski Y., Lanz T. (eds.) 18th Advanced Course of the Swiss Society of Astrophysics and Astronomy (Saas-Fee Courses): Radiation in Moving Gaseous Media. Geneva Obs., p. 1
Kudritzki R.P., 1998, In: Aparicio A., Herrero A., Sánchez F. (eds.) VIII Canary Islands Winter School of Astrophysics on Stellar Astrophysics for the Local Group. Cambridge University Press, p. 149
Langer N., 1992, A&A 265, L17
Langer N., Heger A., 1998a, In: II Boulder–Munich Workshop on Properties of Hot, Luminous Stars. ASP Conf. Series Vol. 131, p. 76
Langer N., Heger A., 1998b, A&A 334, 210
Lawrence L.C., Redish V.C., 1965, Publ. R. Obs. Edinburgh 3, 275
Leitherer C., 1998, In: Aparicio A., Herrero A., Sánchez F. (eds.) VIII Canary Islands Winter School of Astrophysics on Stellar Astrophysics for the Local Group. Cambridge University Press, p. 527
Lucy L.B., 1974, AJ 79, 745
Maeder A., 1997, A&A 321, 134
Maeder A., Zahn J.-P., 1998, A&A 334, 1000
Massey P., 1998, In: Aparicio A., Herrero A., Sánchez F. (eds.) VIII Canary Islands Winter School of Astrophysics on Stellar Astrophysics for the Local Group. Cambridge University Press, p. 95
Massey P., Thompson A.B., 1991, AJ 101, 1408
Matthews T.A., Sandage A.R., 1963, ApJ 138, 30
McErlean N.D., Lennon D.J., Dufton P.L., 1998, A&A 329, 613
Meynet G., Maeder A., 1997, A&A 321, 465
Penny L.R., Gies D.R., Bagnuolo Jr. W.G., 1998, In: II Boulder–Munich Workshop on Properties of Hot, Luminous Stars. ASP Conf. Series Vol. 131, p. 392
Redish V.C., Lawrence L.C., Pratt N.M., 1967, Publ. R. Obs. Edinburgh 5, 111
Santolaya-Rey A.E., Puls J., Herrero A., 1997, A&A 488, 512
Schaller G., Schaerer D., Meynet G., Maeder A., 1992, A&AS 96, 269
Schaerer D., Schmutz W., 1994, A&A 288, 231
Schulte D.H., 1956, ApJ 124, 530
Schulte D.H., 1958, ApJ 128, 41
Sellmaier F., Puls J., Kudritzki R.P., et al., 1993, A&A 273, 533
Smith K.C., Howarth I.D., 1998, MNRAS 299, 1146
Talon S., Zahn J.-P., Maeder A., Meynet G., 1997, A&A 322, 209
Torres-Dodgen A.V., Tapia M., Carroll M., 1990, MNRAS 249, 1
Vacca W.D., Garmany C.D., Shull J.M., 1996, ApJ 460, 914
Walborn N.R., 1973, ApJ 180, L35